Calibration Report GI beamline (1-30nm)

PROBA-2 / LYRA

July 2005

Doc. RP-ROB-LYR-0132-GI-July2005

issue Version 1.1
07 September 2005

Prepared by : A. BEN MOUSSA (ROB)
Verified by :
Released by : J-F. HOCHEDEZ

Distribution List

Recipients	Affiliation	Nr. of Copies
LYRA team	CSL, IMO, PMOD, MPS, IEMN, ROB	Email copy

Document Change Record

Issue	Date	Comments
1.1	7 Sept 2005	initial issue

Table of Contents

Reference documents

[RD1] : LYRA_GI_Instrument_Calibration_Plan-V1.3.doc (ROB)

[RD2] : LYRA_Assembly_270705.xls (PMOD)

Scope

The purpose of this report is to summarize/analyse results from the GI calibration campaign at PTB-Bessy II (July 2005).

1 Execution Plan for LYRA

The PTB campaign plan was executed as following:

Activities number	Activities name	Remark
1	Linearity vs Flux at $\lambda_{1,2}$	See RD1
2	Stability vs Time at $\lambda_{1,2}$	"
3	Spectral responsivity	"
4	Homogeneity at $\lambda_{1,2}$	"

2 RESULTS

2.1 Flux Linearity at 10 and 20nm

The linearity was investigated using different aperture stops or by varying the exit slit of the respective monochromator. After varying the beamline power, about half a minute has been allowed to pass before taking data. The offset and the ring current have been corrected.

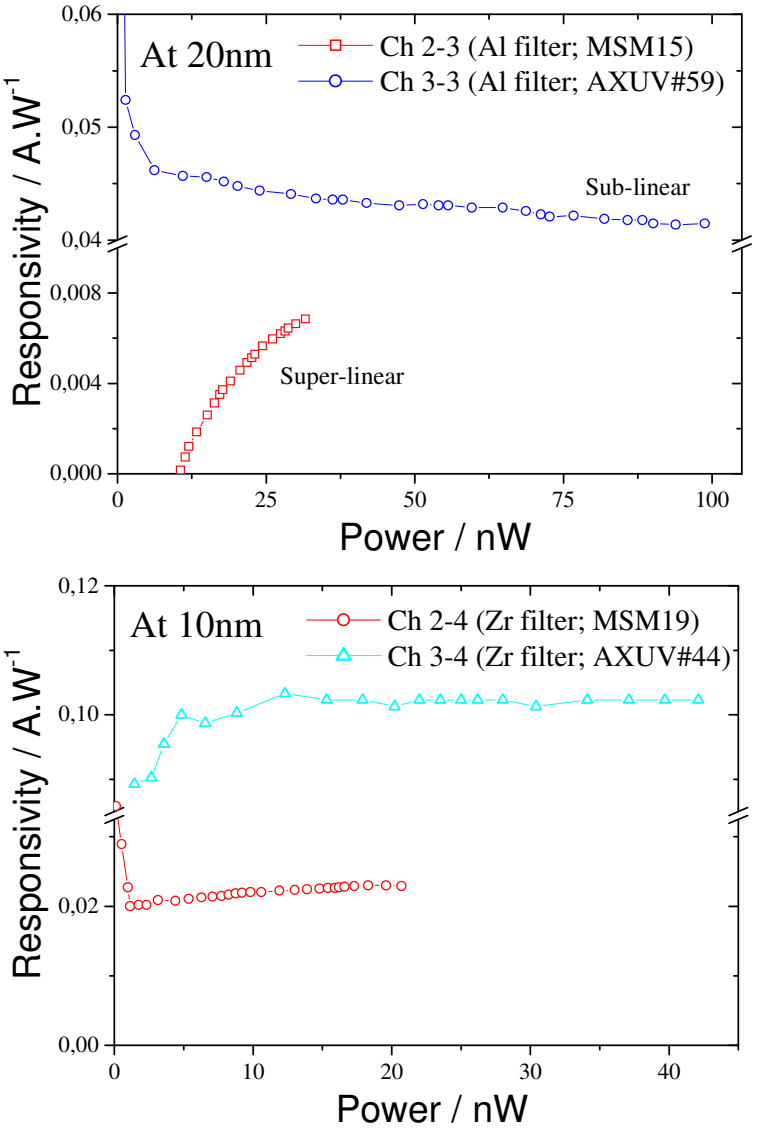

Figure 1. Flux linearity of Al and Zr channels (Response vs. incident power) at 10 and 20 nm. The lines are guides for the eye.

The responsivity of the MSM channels (2-3; 2-4) slightly increases with increasing incident light power indicating a super-linear response. This is in contradiction with the NI measurements on MSM alone where the responsivity decreases with the light power (at 121.6 and 200nm).

For the AXUV channel, the responsivity remains almost constant at 10nm (channel 3-4) indicating a linear response. It slightly decreases at 20nm (channel 3-3) indicating a sublinear response (using a power law as follow: $I = aP^b$; $R \propto P^{b-1}$; $b = 1$ for linear response).

2.2 Stability (Drift) at

The signal stability was measured at 60°C at **10nm** (for Zr channels) and at **18nm** wavelength for Al channels. The shutter was opened and closed as seen in the figure. I corrected the data from the offset and for the small decline of the current of the synchrotron storage ring during the time period of each measurement. Voltage units were changed to current units (A) using the appropriate gain resistor [see RD2]. The expected beam power was calculated using the responsivity data (cf next paragraph).

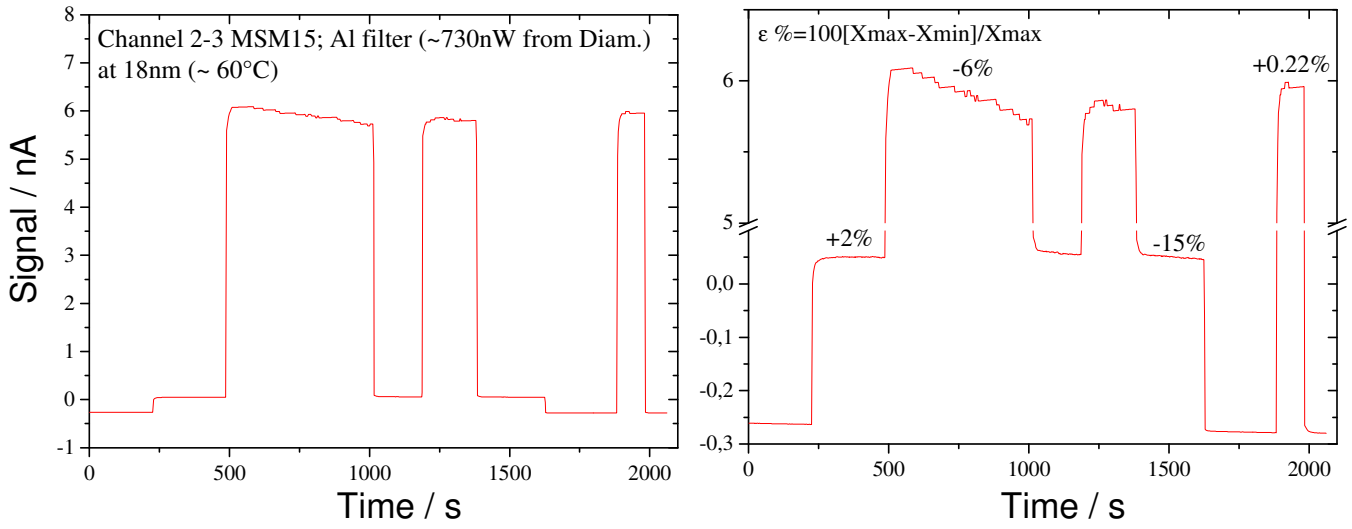

Figure 2. Absolute signal in nA for channels 2-3 as a function of time at 18 nm (left) and close view (right).

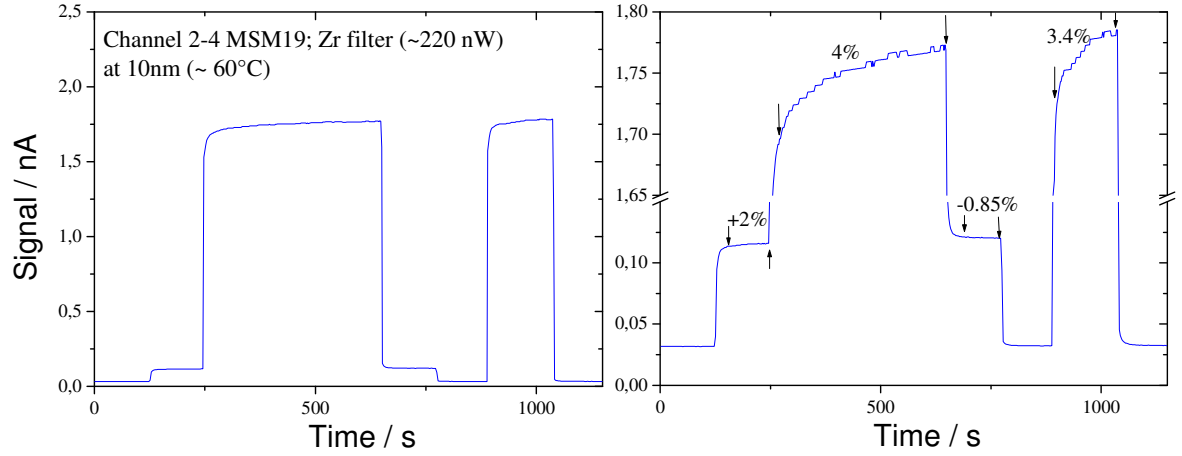

Figure 3. Absolute signal in nA for channels 2-4 as a function of time at 10 nm (left) and close view (right).

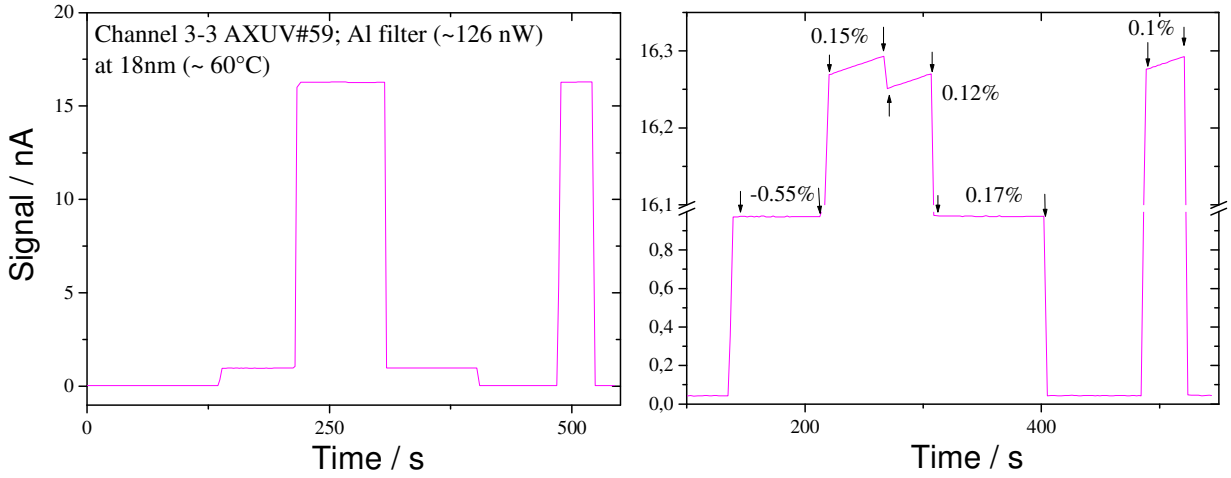

Figure 4. Absolute signal in nA for channels 3-3 as a function of time at 18 nm (left) close view (right).

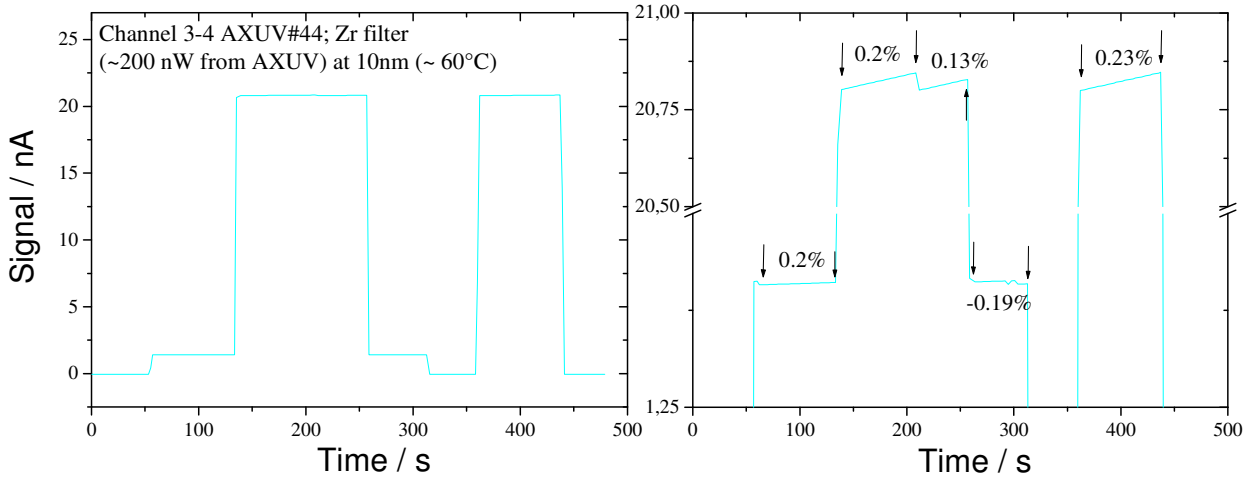

Figure 5. Absolute signal in nA for channels 3-4 as a function of time at 10 nm (left) close view (right).

As seen in the figures, the signal of channel 2-3 (MSM15) decreases with time at full beam power. It looks more stable under low irradiation flux.

The signal of Channel 2-4 (MSM19) increases with time at full beam power. It looks more stable under low irradiation flux too.

Note that the detectors (MSM15 and 19) have the same characteristic alone. The signaldecrease for MSM15 while it increase with MSM19 as a function of time.

For AXUV channels (3-3 and 3-4, the signal increase slightly for a short time then decrease suddenly to increase again. This remains to be explained and may be a concern for LYRA operation.

2.3 Spectral responsivity (1-30nm) and (40-80nm)

The responsivity for LYRA channels were measured in the center position at regular intervals and in finest steps close to C absorption and Al filter cut-off. Voltage units were changed to current units (A) using the appropriate gain resistor [see RD2]. Corrections for offset and ring-current have been applied. We did not plot the estimated error bars to the data since they are negligible.

2.3.1 Channel 2-3 (Al filter, MSM15)

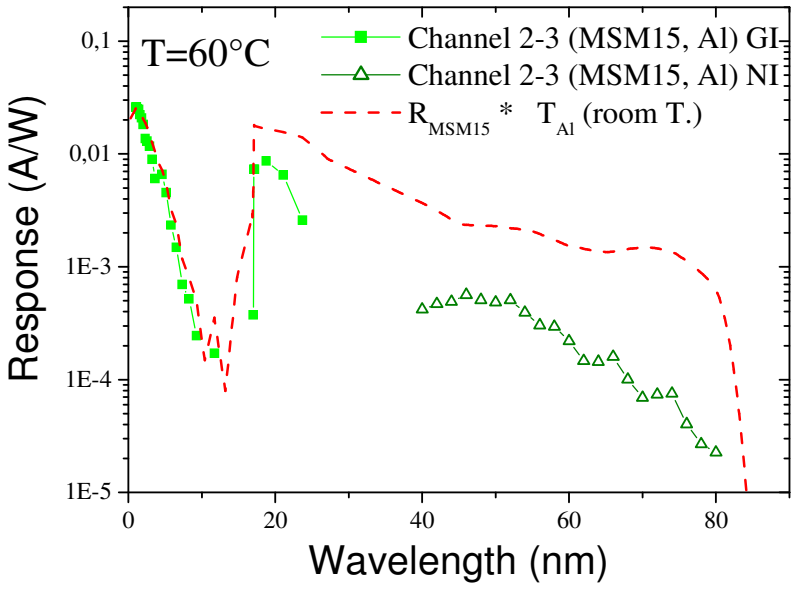

Figure 6. Absolute spectral responsivity (in A/W) of channel 2-3 between 1nm and 80 nm. For comparison, the dotted line represents the model used in the LYRA radiometric model (detector R x Filter T).

2.3.2 Channel 3-3 (Al filter, AXUV #59)

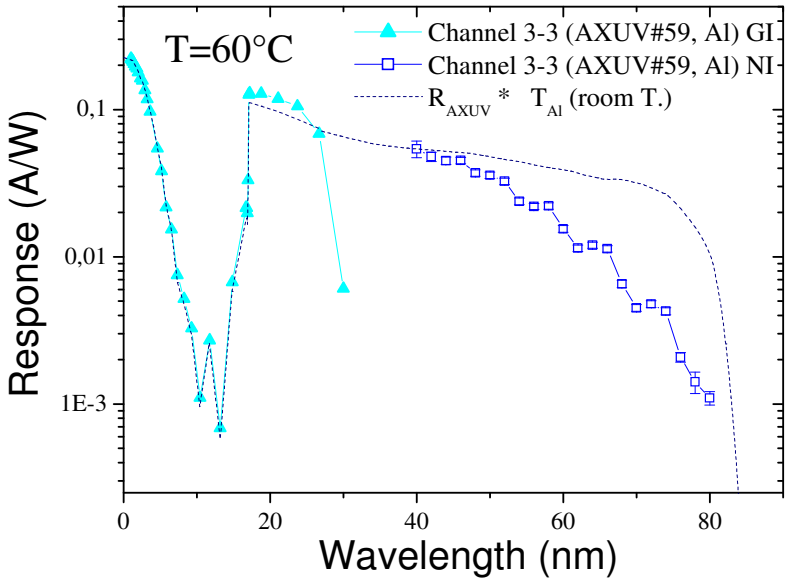

Figure 7. Absolute spectral responsivity (in A/W) of channel 3-3 between 1nm and 80 nm. For comparison, the dotted line represents the model used in the LYRA radiometric model (detector R x Filter T).

2.3.3 Channel 2-4 (Zr filter, MSM19)

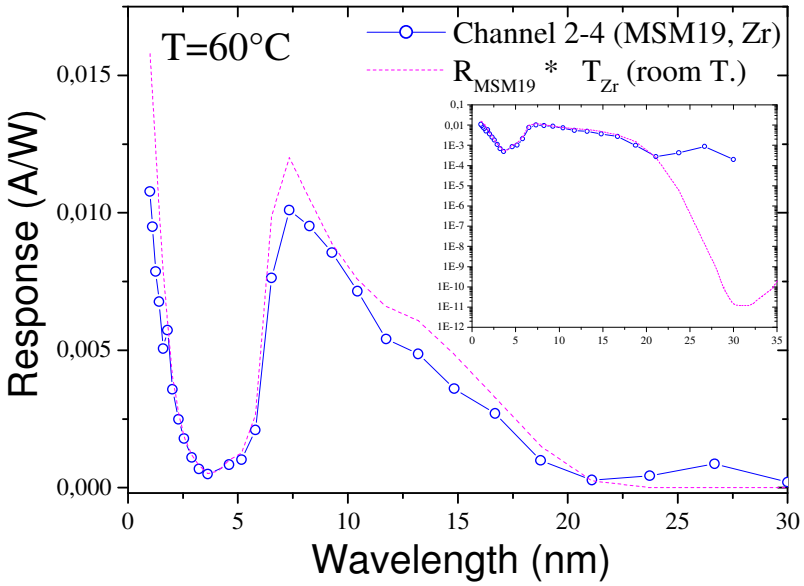

Figure 8. Absolute spectral responsivity (in A/W) of channel 2-4 between 1nm and 30 nm. For comparison, the dotted line represents the model used in the LYRA radiometric model (detector R x Filter T).

2.3.4 Channel 3-4 (Zr filter, AXUV#44)

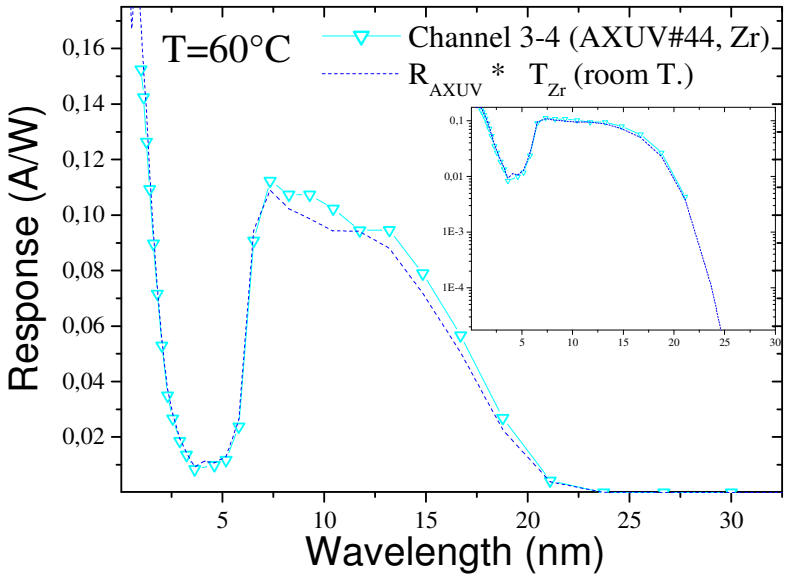

Figure 9. Absolute spectral responsivity (in A/W) of channel 3-4 between 1nm and 30 nm. For comparison, the dotted line represents the model used in the LYRA radiometric model (detector R x Filter T).

Fig 6 to 9 will be analysed in detail by ROB.

Table 1 summarizes the derived results using the TIME-SEE solar spectrums. More information can be found in the updated LYRA radiometric model web site.

http://lyra.oma.be/radiometric_model/radiometric_model.php

Table 1: Expected output signals and purities (width 1-20nm for Zr and 17-70nm for Al) in LYRA channels for minimum solar activity conditions.

Expected SIGNAL and Purity			at Solar Min using Bessy-GI+NI	at Solar Min Radiometric Model
HEAD 2	Channel 3	Al + MSM15	56.8 pA [52.6%]	127.49 pA [73%]
	Channel 4	Zr + MSM19	93.44pA [98.9%]	111.17 pA [99.4%]
HEAD 3	Channel 3	Al + AXUV59	838.7pA [69%]	963.3 pA [71%]
	Channel 4	Zr + AXUV44	1386pA [98.1%]	1344 pA [99.2%]

Data, measured between 1-30nm for Zr and 1-80nm for Al channel, fit with our radiometric model. Here also we rather have an upper limit since not the entire UV and visible spectrum is taken into account.

To be analysed in detail by ROB.

3 Homogeneity

Homogeneity was measured in two perpendicular directions at 1 and 18nm for Al channels (2-3 and 3-3), and at 1 and 10nm for Zr channels (2-4 and 3-4) where "horizontal" means the long side of the LYRA instrument and "vertical" the short side (opposite at NI). The offset voltages are subtracted. I normalized the data to aid comparison. The beamline power has been readjusted between scans to better conform to detector sensitivities.

3.1 HEAD 1: Ch 1-3; 1-4

Waiting DATA from PTB-Bessy at GI

3.2 HEAD 2: Ch 2-3; 2-4

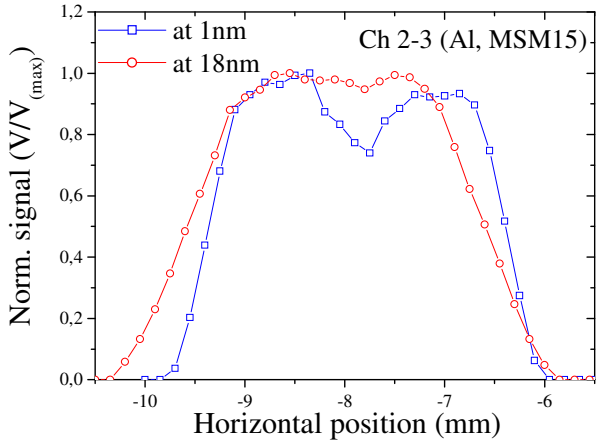

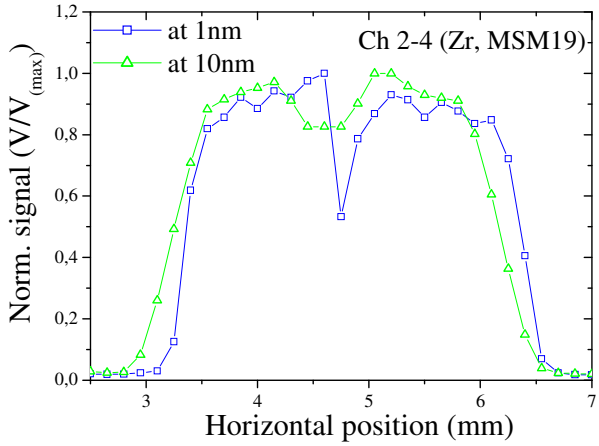

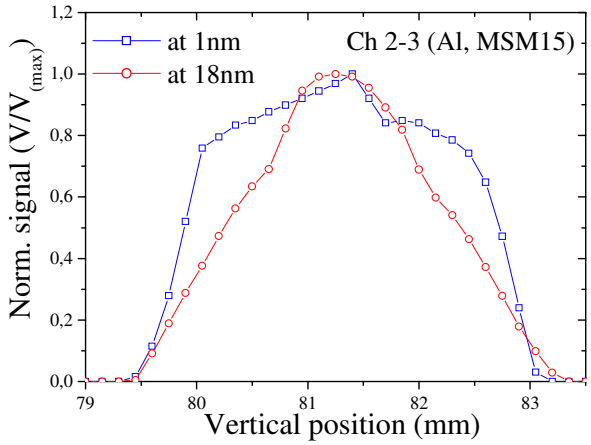

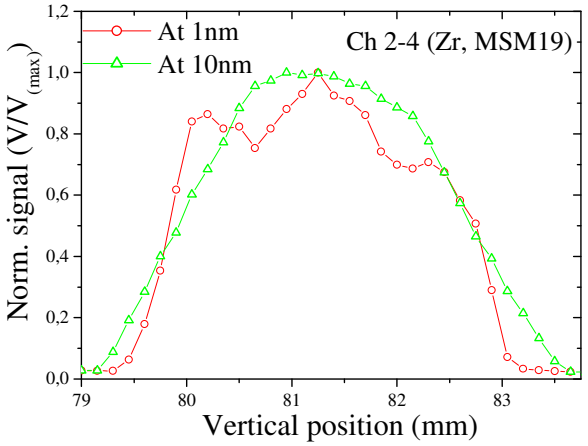

MSM15-Al filter (Ch 2-3) **MSM19-Zr filter (Ch 2-4)**

3.3 HEAD 3: Ch 3-3; 3-4

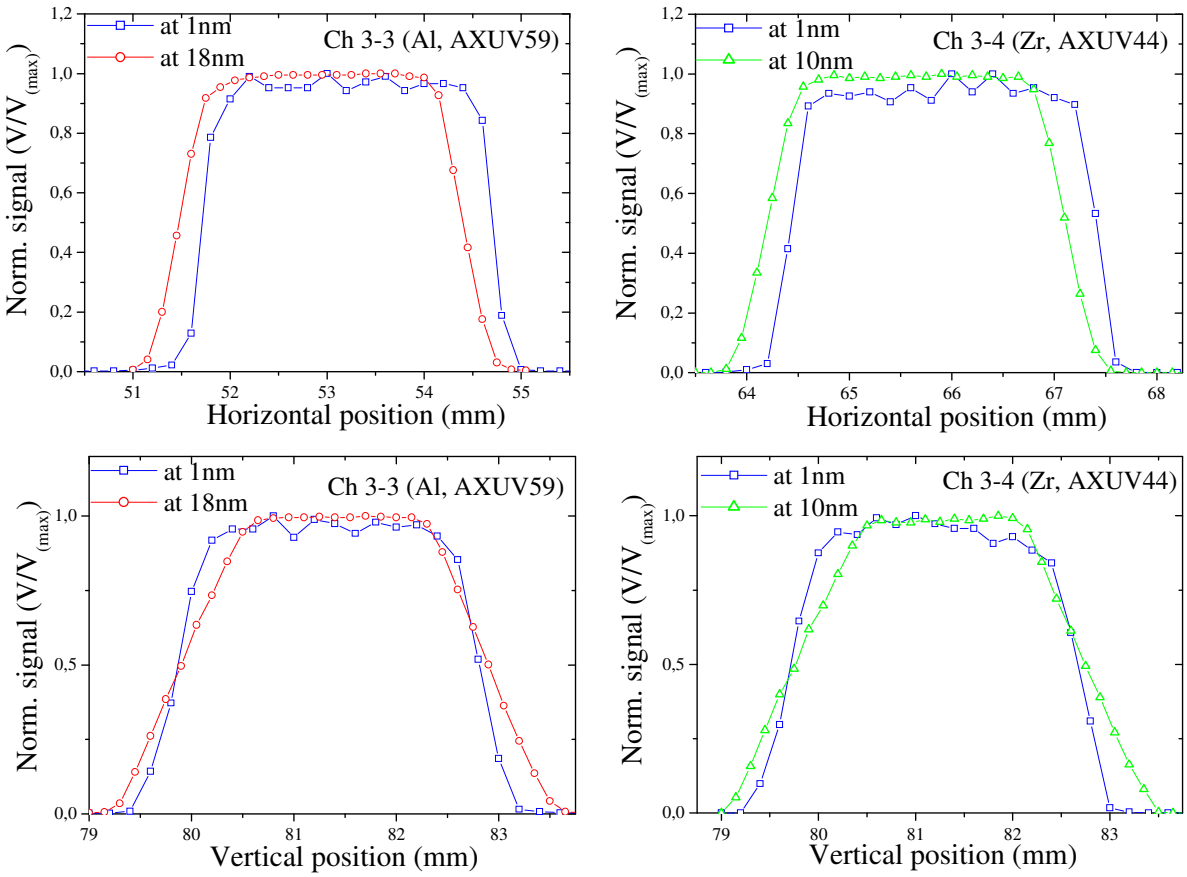

AXUV#59-Al filter (Ch 3-3) **AXUV#44-Zr filter (Ch 3-4)**

Note that the full beam size (0.3 x 0.3 mm) on the measured profile can be negligible.

4 CONCLUSION

Channels (1-3 and 1-4):

No data available at GI

Channels (2-3 and 2-4) MSM:

MSM diamond detectors at GI show a better stability than at Ly-α. Both of them are reasonably uniform (20% deviation) at dedicated wavelength with a sharp dip in sensitivity at the centre of the detector (due to the middle Ti/Pt/Au contact).

Channels (3-3 and 3-4) AXUV:

For the AXUV channel, the responsivity remains almost constant at 10nm (channel 3-4) indicating a linear response. It slightly decreases at 20nm (channel 3-3) indicating a sublinear response. The silicon AXUV#59 and 44 diode look stable after long photon flux exposure (at T=60°C) and uniform. According to the new radiometric model, these channels give a good expected signal and purity.

5 ANNEXE

Using the hypothesis than the detector's response measured last year are correct, we can deduced the Al and Zr filter's transmittance from the different LYRA channels.

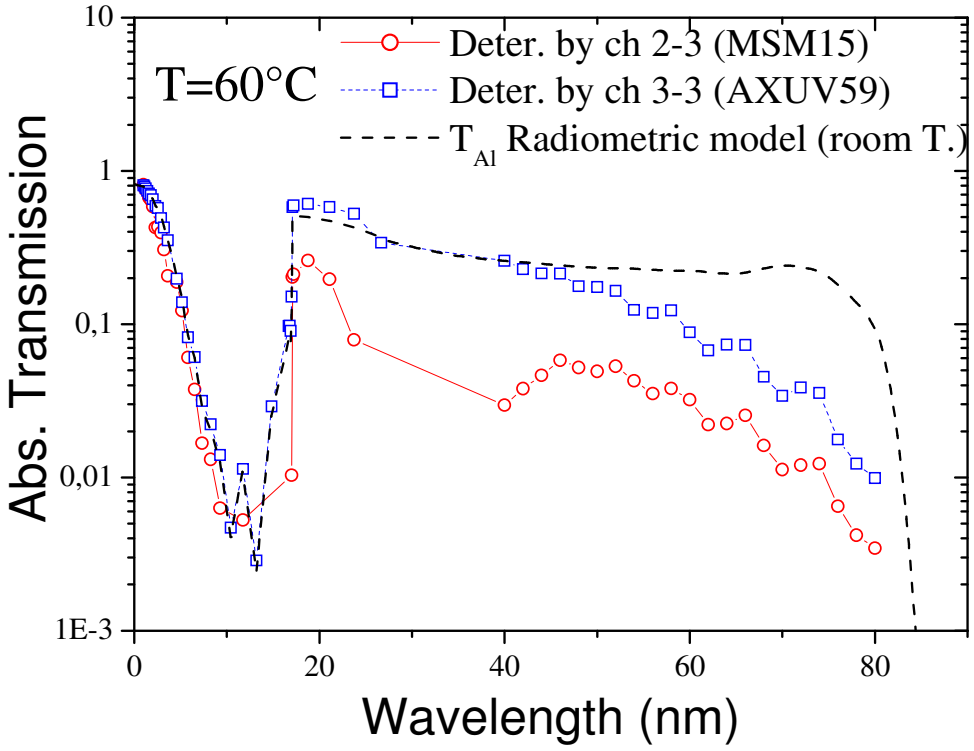

Figure 10. Absolute transmittance of the Al filter deduced from channel 2-3, 3-3 between 1nm and 80 nm. For comparison , the dotted line represents the model used in the LYRA radiometric model (calibrated data at GI range).

As seen in the figure, the Al filter transmission deduced from MSM15 response is very low (by a factor 2-3). It should be notice that the responsivity of MSM15 vary strongly with the incident input power.

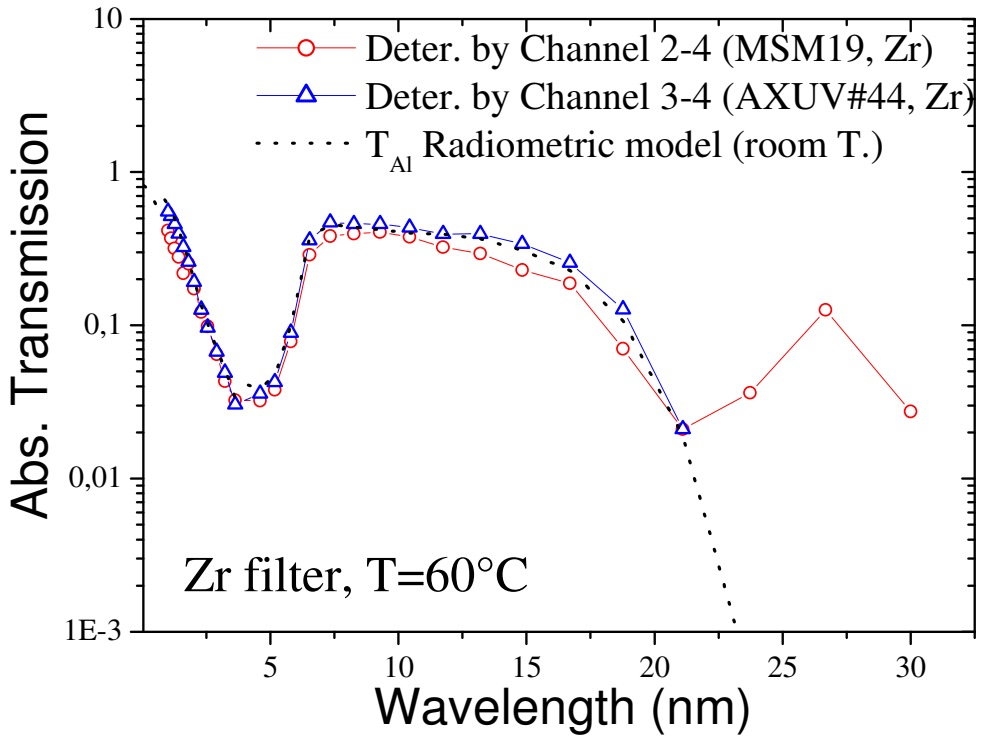

Figure 11. Absolute transmittance of the Zr filter deduced from channel 2-4, 3-4 between 1nm and 30 nm.

For the Zr filter transmission graph, the data fit well with the radiometric model. The incident input power was probably rather close to that used for the MSM19 detector alone. The data up to 22.5nm can not be explained yet.